Analysis and Control of Particulate Processes with Input Constraints

Nael H. El-Farra, Timothy Y. Chiu, and Panagiotis D. Christofides
Dept. of Chemical Engineering, University of California, Los Angeles, CA 90095

A general methodology is proposed for the analysis and control of spatially-homogeneous particulate processes with input constraints modeled by population balance equations. A nonlinear model reduction procedure based on the method of weighted residuals is used for the construction of finite-dimensional ordinary differential equation (ODE) systems that accurately reproduce the dominant dynamics of the particulate process. These ODE systems are used to analyze the limitations imposed by input constraints on the ability to modify the dynamics of the particulate process, leading to an explicit characterization of the set of admissible set points that can be achieved in the presence of constraints. This information, together with the derived ODE systems, is then used as the basis for the synthesis of practically-implementable nonlinear bounded output feedback controllers with well-characterized constraint-handling capabilities. The designed controllers enforce exponential stability in the closed-loop system and achieve particle-size distributions with desired characteristics in the presence of active input constraints. Precise closed-loop stability conditions are given and controller implementation issues are addressed. This method is successfully used to regulate a continuous crystallizer with constrained control action at an open-loop, unstable equilibrium point.

Introduction

Particulate processes are characterized by material domains that are comprised of a continuous phase and a dispersed phase, and are essential in making many high-value industrial products. Examples include the crystallization of proteins for pharmaceutical applications, the emulsion polymerization reactors for the production of latex, and the titania powder aerosol reactors used in the production of white pigments. It is now well understood that the physicochemical and mechanical properties of materials made with particulates depend heavily on the characteristics of the corresponding particle-size distribution (PSD) (for example, a nearly monodisperse PSD is required for titania pigments to obtain the maximum hiding power per unit mass). Therefore, the problem of synthesizing and implementing high-performance model-based feedback control systems on particulate processes to achieve PSDs with desired characteristics has significant industrial value.

Fundamental modeling of particulate processes is usually addressed within the framework of population balances, which allow the derivation of systems of nonlinear partial integro-differential equations that describe the rate of change of the PSD. The population balances are coupled with material and energy balances that describe the rate of change of the state variables of the continuous phase (these are usually systems of nonlinear differential equations which include integrals over the entire particle-size spectrum), leading to complete particulate process models. There is a large body of literature on the development of solution methods and the understanding of dynamics of population balance models (Friedlander, 1977; Gelbard and Seinfeld, 1978; Ramkrishna, 1985; Hill and Ng, 1996; Jerauld et al., 1983; Rawlings and Ray, 1987; Kumar and Ramkrishna, 1996a,b; Nicmanis and Hounslow, 1998). On the other hand, research on control of particulate processes has mainly focused on the understanding of fundamental control-theoretic properties (controllability and observability) of population balance models (Semino and Ray, 1995a) and the application of conventional control schemes (such as proportional-integral and proportional-integral-derivative control, self-tuning control) to crystallizers and emulsion polymerization processes (Semino and Ray,

Correspondence concerning this article should be addressed to P. D. Christofides.

1995b; Rohani and Bourne, 1990; Dimitratos et al., 1994). Results on population balance model-based control of particulate processes include an optimization-based control method developed by Eaton and Rawlings (1990) and successfully applied to a batch crystallization process, as well as nonlinear state feedback control of a cell culture in Kurtz et al. (1988). In Chiu and Christofides (1999), a general model reduction procedure, based on a combination of the method of weighted residuals and approximate inertial manifolds, was developed that allows deriving ordinary differential equation (ODE) approximations of particulate process models, which were used for the synthesis of finite-dimensional output feedback controllers that can be readily implemented in practice. The method was successfully implemented on a continuous crystallizer. These results were extended to particulate processes with time-varying uncertain variables and unmodeled actuator/sensor dynamics in Chiu and Christofides (2000).

Even though the above methods lead to the systematic design of practically implementable nonlinear model-based feedback controllers for particulate processes, they do not deal with the problem of constraints on the capacity of the control actuators. This is an important limitation of these methods, especially in view of the fact that the capacity of control actuators used to regulate particulate processes is almost always limited. Such limitations may arise naturally due to the finite capacity of control actuators (such as bounds on the magnitude of the opening of valves) or may be imposed on the manipulated input to insure safe process operation, meet environmental regulations, or maintain desired product quality specifications. Input constraints restrict our ability to freely modify the dynamic behavior of particulate processes, and the ill-effects due to actuator constraints manifest themselves, for example, in the form of sluggishness of response and loss of stability. Additional problems that arise in the case of dynamic controllers include undesired oscillations and overshoots, a phenomenon usually referred to as "windup".

Recognition of the detrimental effects of input constraints on the stability and performance of chemical processes in general has motivated many recent studies on the dynamics and control of chemical processes subject to input constraints. Notable contributions in this regard include controller design and stability analysis within the model predictive control framework (Rawlings, 1999; Schwarm and Nikolaou, 1999), constrained quadratic-optimal control (Chmielewski and Manousiouthakis, 1998), the design of "anti-windup" schemes in order to prevent excessive performance deterioration of an already designed controller when the input saturates (Kothare et al., 1994; Oliveira et al., 1995; Valluri and Soroush, 1998) the study of the nonlinear bounded control problem for a class of two and three state chemical reactors (Alvarez et al., 1991), and some results on the dynamics of constrained nonlinear systems (Colonius und Kliemann, 1993; Kapoor and Dauotidis, 1999).

This work focuses on the development and application of a general methodology for the analysis and control of constrained spatially-homogeneous particulate processes modeled by population balance equations. Initially, a nonlinear model reduction procedure based on the method of weighted residuals is presented for the construction of finite-dimensional ODE systems that accurately reproduce the dominant dynamics of the particulate process. These ODE systems are then used to analyze the limitations imposed by input constraints on the ability to modify the dynamics of the particulate process, leading to an explicit characterization of the set of admissible set points that can be achieved in the presence of constraints. This information, together with the derived ODE systems, are then used as the basis for the synthesis of practically-implementable nonlinear bounded output feedback controllers that enforce exponential stability in the closed-loop system and achieve PSD with desired characteristics in the presence of active input constraints. Precise closed-loop stability conditions are given and controller implementation issues are addressed. The proposed methodology is successfully applied to a continuous crystallizer.

Preliminaries

Particulate process model with input constraints

We focus on spatially homogeneous (well-mixed) particulate processes with simultaneous particle growth, nucleation, agglomeration and breakage and consider the case of a single internal particle coordinate, which is assumed to be the particle size. Applying a population balance to the particle phase, as well as material and energy balances to the continuous phase, we obtain the following general nonlinear system of partial integro-differential equations

$$\frac{\partial n}{\partial t} = -\frac{\partial[G(x,r)n]}{\partial r} + w(n,x,r), \quad n(0,t) = b[x(t)]$$

$$\dot{x} = f(x) + g(x)\mathrm{sat}[u(t)] + A\int_0^{\tau_{\max}} a(n,r,x)\,dr \qquad (1)$$

where $n(r,t) \in [L_2[0,\ r_{\max}),\ \mathbb{R}]$ is the size distribution function which is assumed to be a continuous and sufficiently smooth function of its arguments (we use the symbol $L_2[0, r_{\max})$ to denote a Hilbert space of continuous functions defined on the interval $[0, r_{\max})$), $r \in [0, r_{\max})$ is the particle size ($r_{\max}$ is the maximum particle size, which may be infinity), t is the time, $x \in \mathbb{R}^n$ is the vector of state variables which describe properties of the continuous phase (such as solute concentration, temperature and pH in a crystallizer), $u(t) = [u_1(t)\ u_2(t)\ \cdots\ u_m(t)]^T \in \mathbb{R}^m$ is the vector of manipulated inputs, and sat refers to the saturation function defined by

$$\mathrm{sat}(u_i) = \begin{cases} u_{i,\min} & \text{if} \quad u_i < u_{i,\min} \\ u_i & \text{if} \quad u_{i,\min} \le u_i \le u_{i,\max} \\ u_{i,\max} & \text{if} \quad u_i > u_{i,\max} \end{cases} \qquad (2)$$

where $u_i \in \mathbb{R}$ and for a vector $u \in \mathbb{R}^m$, $\mathrm{sat}(u) = [\mathrm{sat}(u_1)\ \mathrm{sat}(u_2) \cdots \mathrm{sat}(u_m)]^T$. The presence of the sat operator in Eq. 1 signifies the presence of hard constraints on the manipulated input. Such constraints may arise naturally due to inherent limitations on the capacity of control actuators used to regulate particulate processes or may be imposed for economic or safety reasons.

In Eq. 1, the n-equation is the population balance where $G(x,r)$ is the growth rate that accounts for particle growth through condensation, and $w(n, x, r)$ is a term that accounts for the net rate of introduction of new particles into the system (it includes all the means by which particles appear or disappear within the system including particle agglomeration,

breakage, nucleation, feed, and removal). The x-subsystem of Eq. 1 is derived by applying material and energy balances to the continuous phase. In this subsystem, $f(x)$, $a(n,r,x)$ are smooth nonlinear vector functions, $g(x)$ is a nonlinear matrix function, and A is a constant matrix. The term $A\int_0^{r_{\max}} a(n,r,x)dr$ represents mass and heat transfer from the continuous phase to all the particles in the population.

We define a vector of controlled outputs to express the various control objectives (such as regulation of total number of particles, mean particle size, temperature, pH, and so on) as

$$y_i(t) = h_i\left[\int_0^{r_{\max}} c_\kappa(r)n(r,t)dr, x\right], \quad i = 1, \ldots, m, \quad \kappa = 1, \ldots, l \quad (3)$$

where $y_i(t)$ is the ith controlled output, $h_i(\int_0^{r_{\max}} c_\kappa(r)n(r,t)dr, x)$ is a nonlinear scalar smooth function of its arguments, and $c_\kappa(r)$ is a known smooth function of r which depends on the desired performance specifications. To simplify the notation in our theoretical development, we will not consider measured outputs separately from controlled outputs, which means that we need to assume the availability of online measurements of the controlled output $y_i(t)$.

Throughout the article, the order of magnitude and Lie derivative notations will be needed in our development. In particular, $\delta(\epsilon) = O(\epsilon)$ if there exist positive real numbers $\bar{k}_1$ and $\bar{k}_2$ such that: $|\delta(\epsilon)| \le \bar{k}_1|\epsilon|$, $\forall |\epsilon| < \bar{k}_2$, and $L_f\bar{h}$ denotes the standard Lie derivative of a scalar function $\bar{h}(x)$ with respect to the vector function $f(x)$, $L_f^k\bar{h}$ denotes the k-th order Lie derivative, and $L_gL_f^{k-1}\bar{h}$ denotes the mixed Lie derivative where $g(x)$ is a vector function. We will also need the definition of a class KL function. In particular, a function $\beta(s,t)$ is said to be of class KL if, for each fixed t, the function $\beta(s,\cdot)$ is continuous, increasing, and zero at zero and, for each fixed s, the function $\beta(\cdot,t)$ is nonincreasing and tends to zero at infinity.

Motivating example: a continuous crystallizer

Crystallization is a particulate process that is widely used in industry and requires a population balance to be accurately described, analyzed, and controlled. Crystallizers typically exhibit oscillatory behavior which suggests the use of feedback control to ensure stable operation and attain a crystal-size distribution with desired characteristics. However, one of the biggest problems that hinder the effective implementation of conventional feedback controller design methods is the presence of hard constraints on the manipulated input. Input constraints restrict our ability to modify the dynamics of the process in the desired manner. In order to motivate our discussion on the problem of input constraints and the approach that we propose for dealing with this problem (detailed in the next section), we highlight first in this section, by means of a continuous crystallizer example, some of the key issues that need to be addressed for the effective control of particulate processes with input constraints. In particular, we demonstrate some of the fundamental limitations imposed by input constraints on our ability to steer particulate process dynamics, as well as some of the detrimental effects of input constraints on the performance of conventional feedback controller designs. To this end, we consider the isothermal continuous crystallizer example studied in Chiu and Christofides (1999). The mathematical model for this crystallizer is given by

Table 1. Process Parameters and Dimensionless Variables

$c_0 = 1{,}000.0$	$\mathrm{kg\cdot m^{-3}}$
$c_s = 980.2$	$\mathrm{kg\cdot m^{-3}}$
$\rho = 1{,}770.0$	$\mathrm{kg\cdot m^{-3}}$
$\tau = 1.0$	h
$k_1 = 5.065\times10^{-2}$	$\mathrm{mm\cdot m^3\cdot kg^{-1}\cdot h^{-1}}$
$k_2 = 7.958$	$\mathrm{mm^{-3}\cdot h^{-1}}$
$k_3 = 1.217\times10^{-3}$	
$\sigma = 1.0$	mm
$Da = 200.0$	
$F = 3.0$	
$\alpha = 40.0$	

$$\frac{\partial n}{\partial \tilde{t}} = -k_1(c-c_s)\frac{\partial n}{\partial r} - \frac{n}{\tau} + \delta(r-0)\bar{\epsilon}k_2 e^{-\frac{k_3}{\left(\frac{c}{c_s}-1\right)^2}}$$

$$\frac{dc}{d\tilde{t}} = \frac{(c_0-\rho)}{\bar{\epsilon}\tau} + \frac{(\rho-c)}{\tau} + \frac{(\rho-c)}{\bar{\epsilon}}\frac{d\bar{\epsilon}}{d\tilde{t}} \quad (4)$$

where $n(r,\tilde{t})$ is the number of crystals of radius $r \in [0,\infty)$ at time $\tilde{t}$ per unit volume of suspension, τ is the residence time, c is the solute concentration in the crystallizer, c_0 is the solute concentration in the feed, $\bar{\epsilon} = 1 - \int_0^\infty n(r,\tilde{t})\frac{4}{3}\pi r^3 dr$ is the volume of liquid per unit volume of suspension, c_s is the concentration of solute at saturation, k_1, k_2, and k_3 are constants, and $\delta(r-0)$ is the standard Dirac function. The term containing the Dirac function in Eq. 4 accounts for the production of crystals of infinitesimal (zero) size via nucleation. The parameters used for this crystallizer process model are given in Table 1. It was shown in Chiu and Christofides (1999) that this crystallizer exhibits highly oscillatory behavior resulting from the interplay between the growth and the nucleation terms in the population balance (unstable steady state surrounded by a stable limit cycle).

The control objective is to stabilize the crystallizer and achieve a crystal-size distribution with desired mass by manipulating the solute feed concentration. The manipulated input is therefore taken to be $u(t) = (c_0 - c_{0s})/(c_0 - c_s)$, where c_{0s} is steady-state solute feed concentration, and the controlled output is defined as

$$y(\tilde{t}) = 8\pi\sigma^3\int_0^\infty n(r,\tilde{t})dr = \tilde{x}_0 \quad (5)$$

where $\sigma = k_1\tau(c_0 - c_s)$. Note that both are in dimensionless form. To achieve the desired control objective, we implement a conventional proportional-integral (PI) control scheme

$$\frac{d\eta}{dt} = e$$

$$u = K_c\left[e + \frac{1}{\tau_I}\eta\right] \quad (6)$$

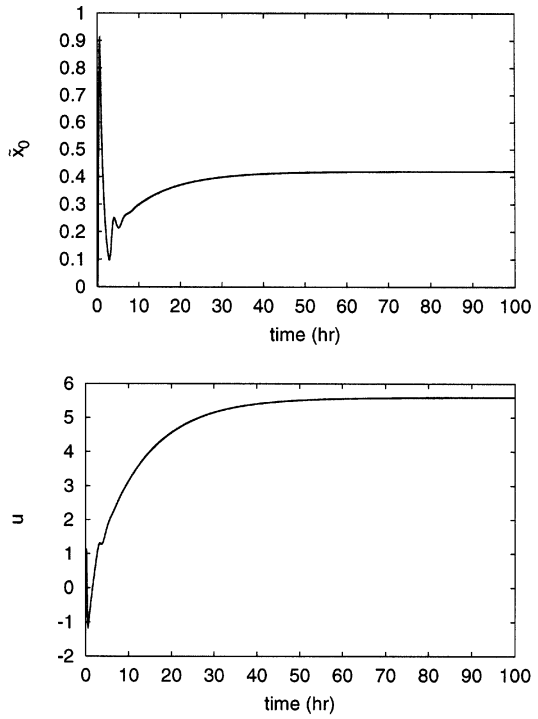

Figure 1. Controlled output (crystal concentration) and manipulated input (solute concentration) profiles under PI control in the absence of input constraints.

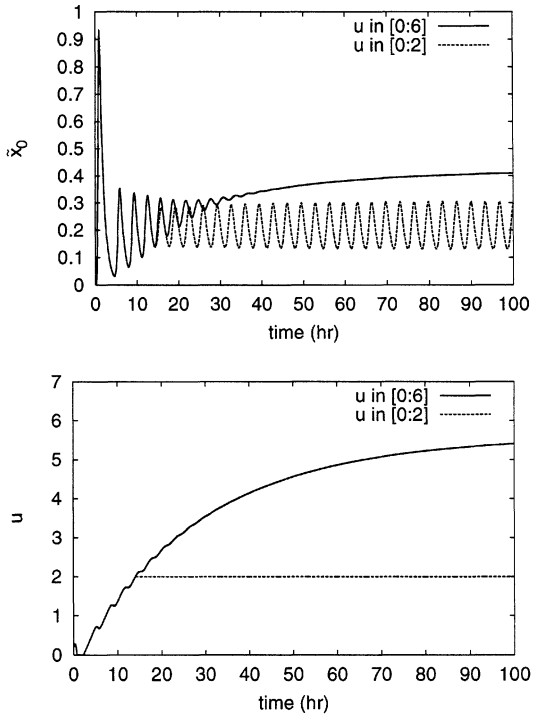

Figure 2. Controlled output (crystal concentration) and manipulated input (solute concentration) profiles under PI control when $u \in [0,2]$ (dashed lines) and when $u \in [0,6]$ (solid lines).

on the crystallizer process model of Eq. 4, where $e = y_{sp} - y$ and u is the controller output. If there are no limits on the maximum solute feed concentration that can be used to achieve the desired control objective, then the controller output and process input are the same. However, suppose that there are limitations on the maximum solute feed concentration, that is, $|u| \le u_{\max}$. In this case, if the solute feed concentration calculated by the controller is, for example, higher than $u_{\max}$, then the actual solute concentration fed to the crystallizer will be just $u_{\max}$ leading to a mismatch between the controller output and actual crystallizer input.

Initially, closed-loop simulation runs were performed to test the ability of the PI controller to achieve the desired control objective in the absence of limitations (constraints) on the maximum solute feed concentration. Figure 1 depicts the dimensionless crystal concentration ($\tilde{x}_0$) and dimensionless solute feed concentration (u) profiles for a 0.4 increase in the set point in the absence of any constraints on the manipulated input (that is, $|u| < \infty$). It is evident from the figure that the PI controller manages eventually to drive the output to its new set point. In contrast, Figure 2 depicts the closed-loop response to the same 0.4 increase in the setpoint in the presence of input constraints. The solid line shows the response when $u \in [0,2]$ and the dashed line shows the response when $u \in [0,6]$. As can be seen from this figure, the PI controller fails (regardless of the PI tuning parameters) to stabilize the crystallizer when the input is constrained in the interval $[0,2]$, leading to sustained oscillations, while it successfully drives the crystallizer output (despite the poor transient performance) to the desired set point when the input is constrained in the interval $[0,6]$.

The contrast between the two different responses in Figure 2 illustrates an example of how input constraints place fundamental limitations on our ability to steer the particulate process to a desired set point under any control law (linear or nonlinear). To understand these limitations, we refer to the input profiles in Figure 2 which show that in order for the process output to reach a set point of 0.4, the process input must reach a steady-state value of 5.3, that is, outside $[0,2]$. Therefore, when the input is constrained in $[0,2]$, the process output cannot accommodate the requested set point change (regardless of the controller used) owing to the fundamental inadmissibility of the desired set point when $u \in [0,2]$. Relaxing the constraints to $[0,6]$ consequently allows the process input to reach a steady-state value of 5.3 and steer the process output to a value of 0.4. Therefore, it is important to keep in mind that this problem of set point inadmissibility is independent of the controller used and cannot be remedied simply by choosing another controller in place of the PI controller.

The prior reasoning immediately raises the following important question: given our knowledge of the constraints on the process input, how can we identify *a prior* (before controller implementation and without running closed-loop simulations) whether a given set point is admissible? It is clear from Figure 2 that lack of this information can easily lead to a poor (that is, inadmissible) choice of the set point and subsequent instability. In the absence of this information, it may not even be clear what the underlying cause of instability is.

This, is turn, may prompt the control engineer to suspect the particular controller used and consequently waste time and effort in retuning the controller or trying other control schemes without realizing that the problem is one that cannot be solved by any controller and is due rather to the inherent limitations, imposed by the constraints. These considerations motivate the need for a systematic approach that explicitly characterizes the limitations imposed by input constraints on our ability to steer the particulate process in a desired direction. Such an approach is needed to provide process operators with the necessary knowledge of which set point changes are feasible and can be achieved in the presence of known constraints on the manipulated input, *independent of the specific control scheme to be used*. The *a priori* availability of this kind of feasibility information is a prerequisite for any effective controller design method that can successfully address the problems caused by input constraints on the operation of the process.

Another important issue that the above crystallizer example highlights is that of the particular choice of the controller to achieve the desired control objective, once that objective is determined to be admissible. Recall from Figure 2 (solid line) that, although the set point is admissible when $u \in [0, 6]$ and that the PI controller stabilizes the process there, the transient performance is poor (compare with Figure 1). This performance deterioration is a direct consequence of input saturation for about 2h in the beginning of the crystallizer operation leading to a more sluggish and oscillatory response. While it is possible to reduce the response settling time by further retuning of the PI controller, this comes at the expense of an unreasonably large overshoot in the process output. It is important to point out here that owing to the complex nonlinear dynamics of the crystallizer, the presence of input constraints, and the large set point change considered, there are no systematic guidelines for tuning the PI controller. Instead, the PI controller was tuned through extensive trial and error to obtain the best possible performance that yields reasonable overshoot (compared to that of the nonlinear controller shown later in Figure 6).

The "traditional" approaches of designing/tuning the PI controller on the basis of a linearized model of the process are inadequate, because they do not account for either the strong nonlinearities present or the input constraints. The performance of any controller designed in this way deteriorates, even in the absence of constraints, as the process moves further away from the steady state around which the model was linearized. In addition to the performance problem, conventional control schemes (such as the PI controller), which are not designed to explicitly handle the presence of input constraints, lack any *a priori* guarantees regarding stability of the constrained closed-loop system starting from a given initial condition. *It is well known that even if a set point is admissible, not every initial condition can be used to reach it.* This initial condition must belong to the region of closed-loop stability. Most conventional control schemes (linear and nonlinear), however, do not provide any systematic way of estimating this region or identifying initial conditions starting from where closed-loop stability is guaranteed in the presence of input constraints. All these considerations combined clearly motivate the need for an alternative, effective, and direct control strategy that can handle the presence of input constraints explicitly in the controller design and provide, simultaneously, an explicit characterization of the region of guaranteed closed-loop stability starting from where the requested stability and performance of the particulate process can be guaranteed in the presence of input constraints.

Motivated by the previous discussion, the development of a rigorous, yet practical, framework for the analysis and control of constrained particulate processes is the subject of this article. We begin in the next section with an outline of the proposed framework, which will serve as the road map for our development throughout the manuscript.

Methodological Framework for Analysis and Control of Constrained Particulate Processes

Owing to its distributed parameter nature, the system of Eq. 1 cannot be used directly as the basis for either the analysis of the limitations imposed by input constraints on particulate process dynamics, or the synthesis of practically implementable (low-order) nonlinear controllers that cope effectively with the problem of constraints. This fact, together with the realization that the dominant dynamics of particulate processes are characterized by a small number of degrees of freedom (Chiu and Christofides, 1999), motivate employing the following methodology for the analysis and control of constrained particulate processes of the form of Eq. 1:

(1) Initially, the method of weighted residuals is used to derive a nonlinear ODE system that accurately reproduces the solutions and dynamics of the system of Eq. 1.

(2) Next, the low-order ODE approximation of the system of Eq. 1 is used as the basis for analyzing the fundamental limitations imposed by input constraints on our ability to modify the dynamics of the particulate process. This is done by identifying the set of admissible set points that can be attained in the presence of the given input constraints.

(3) Then, given the set of feasible control objectives, the low-order ODE approximation of the system of Eq. 1 is used as the basis for the direct synthesis, via Lyapunov techniques, of practically implementable bounded nonlinear output feedback controllers that cope effectively with the problem of input constraints by: (a) enforcing stability and set point tracking in the constrained closed-loop ODE system, and (b) providing an explicit characterization of the set of operating conditions starting from where the desired closed-loop stability and performance are guaranteed in the presence of constraints.

(4) Finally, the resulting closed-loop system (particulate process model of Eq. 1 and controller) is analyzed to derive conditions that guarantee that the desired stability and set point tracking properties are enforced in the infinite-dimensional closed-loop system.

Model Reduction

We initially use the method of weighted residuals to derive a set of nonlinear ODEs that accurately reproduce the solutions and the dominant dynamics of the distributed parameter system of Eq. 1. The central idea of the method of weighted residuals is to approximate the exact solution of $n(r, t)$ by an infinite series of orthogonal basis functions defined on the interval $[0, r_{\max})$ with time-varying coefficients, substitute the series expansion into Eq. 1, and then take the

inner product with respect to a complete set of weighted functions to compute a set of ODEs which describes the rate of change of the time-varying coefficients of the series expansion of the solution. Specifically, we expand the solution of $n(r,t)$ in an infinite series in terms of an orthogonal and complete set of basis functions $\phi_k(r)$, where $r \in [0, r_{\max})$, $k = 1, \ldots, \infty$, as follows

$$n(r,t) = \sum_{k=1}^{\infty} a_k(t)\phi_k(r) \tag{7}$$

where $a_k(t)$ are time-varying coefficients. Substituting the above expansion into the particulate process model of Eq. 1, multiplying the population balance with the weighting functions $\psi_\nu(r)$, integrating over the entire particle-size spectrum and, finally, truncating the series expansion of $n(r,t)$ up to order N and keeping and first N equations (that is, $\nu = 1, \ldots, N$), we obtain the following finite set of ODEs that represent an accurate approximation of the infinite-dimensional system of Eq. 1

$$\begin{aligned}\int_0^{r_{\max}} \psi_\nu(r) \sum_{k=1}^{N} \phi_k(r) \frac{\partial a_{kN}(t)}{\partial t} dr \\ = -\sum_{k=1}^{N} a_{kN}(t) \int_0^{r_{\max}} \psi_\nu(r) \frac{\partial \left[\left(G(x_N, r)\phi_k(r) \right) \right]}{\partial r} dr \\ + \int_0^{r_{\max}} \psi_\nu(r) w\left[\sum_{k=1}^{N} a_{kN}(t)\phi_k(r),\, x_N,\, r \right] dr,\ \nu = 1, \ldots, N \\ \dot{x}_N = f(x_N) + g(x_N)\mathrm{sat}(u(t)) \\ + A\int_0^{r_{\max}} a\left(\sum_{k=1}^{N} a_{kN}(t)\phi_k(r),\, r,\, x_N \right) dr\end{aligned} \tag{8}$$

where x_N and a_{kN} are the approximations of x and a_k obtained by an N-th order truncation. Introducing the vector notation $a_N = [a_{1N} \cdots a_{NN}]$, and after some rearrangements, Eq. 8 can be cast in the following general form

$$\begin{aligned}\dot{a}_N &= f^*(a_N, x_N) \\ \dot{x}_N &= f(x_N) + g(x_N)\mathrm{sat}(u(t)) \\ &\quad + A\int_0^{r_{\max}} a\left(\sum_{k=1}^{N} a_{kN}(t)\phi_k(r),\, r,\, x_N \right) dr\end{aligned} \tag{9}$$

where the explicit expression of $f^*(a_N, x_N)$ is omitted for brevity. Setting $\tilde{x} = [a_N^T\ x_N^T]^T$, we obtain the following multi-input multi-output finite-dimensional ODE system

$$\begin{aligned}\dot{\tilde{x}} &= \tilde{f}(\tilde{x}) + \sum_{i=1}^{m} \tilde{g}_i(\tilde{x})\mathrm{sat}(u_i) \\ y_{s_i} &= \tilde{h}_i(\tilde{x}),\quad i = 1, \ldots, m\end{aligned} \tag{10}$$

where $\tilde{f}(\tilde{x})$, $\tilde{g}_i(\tilde{x})$, $\tilde{w}(\tilde{x})$ are nonlinear vector functions whose explicit form is omitted brevity. Using results from singular perturbation theory, the asymptotic validity of the ODE approximation was established in proposition 1 in Chiu and Chritofides (1999).

Remark 1. In the series expansion of Eq. 7, the basis, $\{\phi_k\}$, $j = 1, \ldots, \infty$, of $L_2[0, r_{\max})$ can be chosen from standard basis function sets (for example, when $r_{\max} = \infty$, $\{\phi_k\}$ can be chosen to be Laguerre polynomials, in which the method of weighted residuals reduces to the method of moments when the weighting functions are chosen as $\psi_\nu = r^\nu$), or it can be computed by applying Karhunen-Loève expansion on an appropriately chosen ensemble of solutions of the system of Eq. 1.

Remark 2. When an arbitrary set of basis functions is used in the expansion of Eq. 7, the ODE system of Eq. 9 may be of very high order in order to accurately describe the dominant dynamics of the system of Eq. 1, and, therefore, to be suitable for the synthesis of a high-performance nonlinear controller. Unfortunately, high dimensionality of the system of Eq. 9 leads to a complex design and high-order controllers, which cannot be readily implemented in practice. An approach to overcome this problem is to reduce the dimension of the system of Eq. 9 further by utilizing the concept of approximate inertial manifolds for particulate process models proposed in Chiu and Christofides (1999).

Computation of Admissible Set Points

Having obtained a low-order approximate ODE system that accurately reproduces the solution and dominant dynamics of the particulate process, we are now in a position to analyze the limitations imposed by constraints on our ability to modify the dynamics of particulate processes, on the basis of the constrained ODE system of Eq. 10. Particulate processes typically operate at constant set points corresponding to equilibrium points of the closed-loop system (such as a desired total number of particles, mean particle size, and temperature). However, it may not be feasible to steer the closed-loop system to the desired operating point, in the presence of constraints, irrespectively of the choice of the control strategy. Thus, even before designing a control policy, it becomes important to investigate the feasibility of controlling the particulate process at a desired set point in the presence of constraints. Addressing this problem, in its full generality, entails two main tasks. The first task is that of identifying the set of admissible set points that the particulate process can be steered to, in the presence of constraitns. The second task is that of characterizing the set of admissible initial conditions, starting from where a given admissible set point can be reached in the presence of constraints. We will focus on the first task in this section and defer discussion of the second task until later.

To accomplish our goal of identifying the set of admissible set points permitted by input constraints, it is useful to view the constrained ODE system of Eq. 10 as a dynamical system where the control input u_i is viewed as a parameter that takes values in the set of admissible control inputs, that is, the interval $U_i = [u_{i,\min}, u_{i,\max}]$. In other words, we consider the following unforced system

$$\dot{\tilde{x}} = \tilde{f}(\tilde{x}) + \sum_{i=1}^{m} \tilde{g}_i(\tilde{x})u_i^0,\quad i = 1, \ldots, m \tag{11}$$

obtained from the system of Eq. 10 for a constant value of u_i denoted by $u_i^0 \in U_i$. An immediate consequence of this view is the realization that the presence of constraints on the val-

ues that the parameter u_i^0 in the system of Eq. 11 can take leads to natural limitations on the steady states or equilibrium states and, consequently, the set points that the ODE system can attain. Exploiting this fact, the problem of characterizing the limitations imposed by input constraints is equivalent to that of explicitly characterizing the dependence of the equilibrium states of the constrained ODE system of Eq. 11 on the admissible values of u_i^0 dictated by the given input constraints. For a given value of the control input $u_i^0 \in U_i$, one can obtain the admissible equilibrium states of the system of Eq. 10 by solving the following set of algebraic equations

$$0 = \tilde{f}(\tilde{x}_s) + \sum_{i=1}^{m} \tilde{g}_i(\tilde{x}_s) u_i^0, \quad i = 1, \ldots, m \tag{12}$$

where $\tilde{x}_s$ represents the admissible steady state for the above ODE system. As the value of u_i^0 is varied smoothly over the set of admissible control inputs U_i, we obtain the set of all admissible equilibrium points of the constrained ODE system of Eq. 10 that can be attained in the presence of constraints. Finally, the admissible set points can be computed directly from the following relation

$$v_i = \tilde{h}_i(\tilde{x}_s), \quad i = 1, \ldots, m \tag{13}$$

Remark 3. The above analysis provides a systematic and practical method for computing the approximate admissible set points of the constrained particulate process of Eq. 1 on the basis of the ODE system of Eq. 10. The only task involved in this method is the solution of a small (due to the low-dimensional nature) set of algebraic equations of the form of Eq. 12 as u_i^0 takes values in the set of admissible control inputs. Note that this analysis is independent of the specific control strategy that one may wish to implement, and that this analysis does not provide any information regarding from where, in state-space, a particular admissible set point can be reached. In other words, given an admissible equilibrium point $\tilde{x}_s$ obtained by solving Eq. 12, the above analysis does not say if this point will actually be achieved under a given controller and starting from a given initial condition. The task of providing such information will be addressed in the controller design step of our methodology. What the above analysis allows us to conclude, however, is whether the given input constraints place any fundamental limitations on our ability to reach a particular set point, and can therefore be used by process operators to identify *a prior* (before controller design) admissible control objectives.

Remark 4. Recent research on the dynamical analysis of nonlinear control systems with input constraints (Colonius and Kliemann, 1993) has provided a system-theoretic characterization of the regions of controllability under constraints, the so-called control sets, where *any* two points in state-space can be reached from each other with the available control action. As the range of manipulated input is varied smoothly over a sufficiently small finite range, these control sets emerge and evolve around the equilibrium points of the nominal system of Eq. 11. Although control sets provide a more detailed characterization of the limitations imposed by input constraints on the system dynamics, such a characterization remains largely theoretical and not very useful from a computational standpoint. The construction of control sets is actually a very cumbersome task even for low-dimensional systems (Kapoor and Daoutidis, 1999). On the other hand, computation of the set of admissible set points, contained within a control set, is a relatively straightforward task that is computationally feasible and provides a valuable piece of information at the same time. Note that the concept of using steady-state system analysis to reach certain conclusions about the control of a dynamic system has been discussed also in the context of integration of process design and control (Stephanopoulos, 1983; Fisher et al., 1985).

Let us now apply our feasibility analysis to the continuous crystallizer example considered earlier in the preliminaries section. It was shown in Chiu and Christofides (1999) that upon application of the method of moments to the continuous crystallizer process of Eq. 4 and neglecting moments of order four and higher, one can derive the following dimensionless ODE system that accurately reproduces the dynamics of the distributed process model of Eq. 4

$$\begin{aligned}
\dot{\tilde{x}}_0 &= -\tilde{x}_0 + (1 - \tilde{x}_3)\, Da\, e^{\frac{-F}{\tilde{y}^2}} \\
\dot{\tilde{x}}_1 &= -\tilde{x}_1 + \tilde{y}\tilde{x}_0 \\
\dot{\tilde{x}}_2 &= -\tilde{x}_2 + \tilde{y}\tilde{x}_1 \\
\dot{\tilde{x}}_3 &= -\tilde{x}_3 + \tilde{y}\tilde{x}_2 \\
\dot{\tilde{y}} &= \frac{1 - \tilde{y} - (\alpha - \tilde{y})\tilde{y}\tilde{x}_2}{1 - \tilde{x}_3} + \frac{u}{1 - \tilde{x}_3}
\end{aligned} \tag{14}$$

where

$$\begin{gathered}
t = \frac{\bar{t}}{\tau}, \quad \tilde{x}_0 = 8\pi\sigma^3\mu_0, \quad \tilde{x}_1 = 8\pi\sigma^2\mu_1, \quad \tilde{x}_2 = 4\pi\sigma\mu_2, \\
\tilde{x}_3 = \frac{4}{3}\pi\mu_3, \ \ldots, \ \sigma = k_1\tau(c_0 - c_s), \quad Da = 8\pi\sigma^3 k_2\tau, \\
F = \frac{k_3 c_s^2}{(c_0 - c_s)^2}, \quad \alpha = \frac{(\rho - c_s)}{(c_0 - c_s)}, \quad \tilde{y} = \frac{(c - c_s)}{(c_0 - c_s)}, \\
u = \frac{(c_0 - c_{0s})}{(c_0 - c_s)}
\end{gathered} \tag{15}$$

μ_i is the i-th moment, $\tilde{x}_0$ is a dimensionless crystal concentration, and u is a dimensionless solute feed concentration. Values of the process parameters and the dimensionless variables Da, F, and α are given in Table 1. To compute the admissible set points for this system, we take the set of admissible control inputs to be $U = [0, 6]$. Setting the lefthand side of Eq. 14 equal to zero, we obtain a set of algebraic equations that can be solved for each value of $u \in U$. Figure 3 illustrates the admissible set points for the crystal concentration which can be achieved with the available control inputs. From this figure, the reason for the failure of the PI controller to stabilize the crystallizer in Figure 2 is evident. Allowing the control inputs to vary only in the set [0, 2] renders the requested set point $\tilde{x}_0 = 0.4$ inadmissible. With the aid of Figure 3, this conclusion can now be reached *a priori* without having to implement the controller.

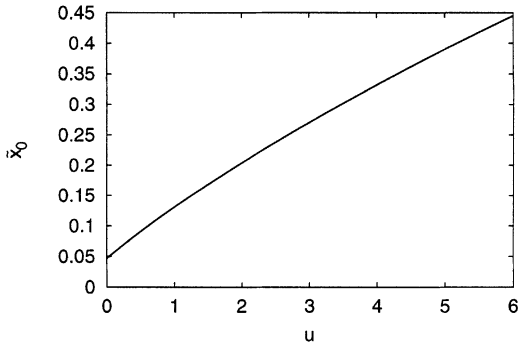

Figure 3. Admissible crystal concentration set points with constrained process input in $u \in [0,6]$.

Bounded Nonlinear Control of Particulate Processes

Having obtained a low-order ODE system that captures the dominant dynamics of the particulate process and identified the set of feasible control objectives that can be achieved in the presence of constraints, we are now motivated to proceed with the third step of our proposed methodology. In this section, we use the constrained low-order ODE system of Eq. 10 as the basis for developing an effective control strategy that handles explicitly the problem of constraints. The key components of this strategy involve: (a) the synthesis of a practically implementable bounded nonlinear output feedback controller that enforces stability and set point tracking in the closed-loop system in the presence of active input constraints, and (b) the explicit characterization of the state-space region of guaranteed closed-loop stability associated with the designed controller. The output feedback controller is constructed through a standard combination of a bounded state feedback controller with a state observer. The state feedback controller is synthesized via Lyapunov-based control methods and the state observer is an extended Luenberger-type observer. Before we proceed with the controller design, we begin in the next subsection with some preliminaries that will be used to state the controller synthesis result.

Preliminaries

Referring to the system of Eq. 10, we define the relative order of the output y_{s_i} with respect to the vector of manipulated inputs u as the smallest integer r_i for which

$$\left[L_{\tilde{g}_1}L_{\tilde{f}}^{r_i-1}\tilde{h}_i(\tilde{x})\cdots L_{\tilde{g}_m}L_{\tilde{f}}^{r_i-1}\tilde{h}_i(\tilde{x})\right] \not\equiv [0\cdots 0] \quad (16)$$

or $r_i = \infty$ if such an integer does not exist. We also define the characteristic matrix

$$C(\tilde{x}) = \begin{bmatrix} L_{\tilde{g}_1}L_{\tilde{f}}^{r_1-1}\tilde{h}_1(\tilde{x}) & \cdots & L_{\tilde{g}_m}L_{\tilde{f}}^{r_1-1}\tilde{h}_1(\tilde{x}) \\ L_{\tilde{g}_1}L_{\tilde{f}}^{r_2-1}\tilde{h}_2(\tilde{x}) & \cdots & L_{\tilde{g}_m}L_{\tilde{f}}^{r_2-1}\tilde{h}_2(\tilde{x}) \\ \vdots & \cdots & \vdots \\ L_{\tilde{g}_1}L_{\tilde{f}}^{r_m-1}\tilde{h}_m(\tilde{x}) & \cdots & L_{\tilde{g}_m}L_{\tilde{f}}^{r_m-1}\tilde{h}_m(\tilde{x}) \end{bmatrix} \quad (17)$$

To proceed with the controller synthesis and under the assumption that the relative degree is well-defined, we transform the system of Eq. 10 into the following partially linear form

$$\begin{aligned} \dot{\zeta}_1^{(i)} &= \zeta_2^{(i)} \\ &\vdots \\ \dot{\zeta}_{r_i-1}^{(i)} &= \zeta_{r_i}^{(i)} \\ \dot{\zeta}_{r_i}^{(i)} &= L_{\tilde{f}}^{r_i}\tilde{h}_i(\tilde{x}) + \sum_{k=1}^{m} L_{\tilde{g}_k}L_{\tilde{f}}^{r_i-1}\tilde{h}_i(\tilde{x})u_k \quad (18) \\ \dot{\eta}_1 &= \Psi_1(\zeta,\eta) \\ &\vdots \\ \dot{\eta}_{(n+N)-\Sigma_i r_i} &= \Psi_{(n+N)-\Sigma_i r_i}(\zeta,\eta) \\ y_{s_i} &= \zeta_1^{(i)}, \quad i=1,\ \ldots,\ m \end{aligned}$$

where $\tilde{x} = T^{-1}(\zeta,\eta)$, $\zeta = [\zeta(1)^T \cdots \zeta^{(m)^T}]^T$, $\eta = [\eta_1 \cdots \eta_{(n+N)-\Sigma_i r_i}]^T$. This transformation is standard in all general nonlinear process control methods whose objective is to force the process output to follow the reference input. Defining the tracking error $e_k^{(i)} = \zeta_k^{(i)} - v_i^{(k-1)}$ and introducing the vector notation $e^{(i)} = [e_1^{(i)} e_2^{(i)} \cdots e_{r_i}^{(i)}]^T$, $e = (e^{(1)^T}\ e^{(2)^T} \cdots e^{(m)^T})^T$, where $i = 1,\ \cdots,\ m$, $k = 1,\ \cdots,\ r_i$, the ζ-subsystem of Eq. 18 can be further transformed into the following more compact form

$$\dot{e} = Ae + B\left[l_1(e,\eta,\bar{v}) + C(\tilde{x})u\right] \quad (19)$$

where A, B, are constant matrices of dimensions $(\Sigma_{i=1}^m r_i)\times(\Sigma_{i=1}^m r_i)$ and $(\Sigma_{i=1}^m r_i)\times m$, respectively, $l_1(e,\ \eta,\ \bar{v})$ is a $(\Sigma_{i=1}^m r_i)\times 1$ continuous nonlinear vector function, and $\bar{v}$ is a vector of the form $\bar{v} = \mathbf{V}(v_i, v_i^{(1)}, \ldots, v_i^{(r_i)})$ where $\mathbf{V}(v_i, v_i^{(1)}, \ldots, v_i^{(r_i)})$ is a smooth vector function, and $v_i^{(k)}$ is the kth time derivative of the external reference input v_i (which is assumed to be a smooth function of time). The specific forms of these functions are omitted for brevity. Finally, we define the function $\tilde{f}(e,\eta,\bar{v}) = Ae + Bl_1(\tilde{x})$, and denote by $\bar{g}_i(e,\eta,\bar{v})$ the i-th column of the matrix function $BC(\tilde{x})$, $i = 1,\ \ldots\ m$.

Controller synthesis

Towards the end goal of synthesizing the necessary bounded nonlinear output feedback controller, we use the nonlinear system of Eq. 18 first to synthesize, via Lyapunov-based control methods, a bounded nonlinear state feedback controller of the general form

$$u = p(\tilde{x},\bar{v}) \quad (20)$$

where $p(\tilde{x},\bar{v})$ is a bounded vector function, that is, $|u| \le u_{\max}$, where $|\cdot|$ is the Euclidean norm that: (a) enforces exponential stability and reference input tracking in the closed-loop system in the presence of active input constraints and (b) provides an explicit characterization of the region in state-space where the previous closed-loop properties are guaranteed.

To construct the desired stabilizing state feedback controller for the system of Eq. 10, we use Lyapunov-based control methods. The basic idea behind any Lyapunov-based controller design is the selection of an appropriate Lyapunov function whose time-derivative can be rendered negative definite, via feedback, along the trajectories of the closed-loop

system. A natural choice for our system, suggested by the partially linear form of Eq. 19, is a quadratic Lyapunov function $V = e^T P e$, where P is a positive definite matrix chosen to satisfy the following Riccati matrix inequality

$$A^T P + PA - PBB^T P < 0 \tag{21}$$

which consequently guarantees the negative definiteness of $\dot{V}$. Using this Lyapunov function, we design a bounded nonlinear state feedback controller of the form

$$u = -\frac{1}{2} R^{-1}(\tilde{x}) \left(L_{\tilde{g}} V\right)^T \tag{22}$$

where $R^{-1}(\tilde{x})$ is a strictly positive nonlinear scalar function whose specific expression is given in Theorem 1 and $L_{\tilde{g}} V$ is a row vector given by $L_{\tilde{g}} V = [L_{\tilde{g}1} V \cdots L_{\tilde{g}_m} V]$. As will be discussed, the bounded nature of the state feedback controller will assist in addressing the problem of constraints by providing an explicit characterization of the set of admissible initial states, starting from where the desired closed-loop properties are guaranteed.

Under the hypothesis that the system of Eq. 10 is locally observable (that is, its linearization around the desired operating steady state is observable), the practical implementation of a nonlinear state feedback controller of the form of Eq. 22 will be achieved by employing the following nonlinear state observer

$$\frac{d\omega}{dt} = \tilde{f}(\omega) + \tilde{g}(\omega)\mathrm{sat}(u) + L\left[y - \tilde{h}(\omega)\right] \tag{23}$$

where ω denotes the observer state vector (the dimension of the vector ω is equal to the dimension of $\tilde{x}$ in the system of Eq. 10), $y = [y_1 \ y_2 \ \cdots y_m]^T$ is the measured output vector, and L is a matrix chosen so that the eigenvalues of the matrix $C_L = \partial \tilde{f}/\partial \omega_{(\omega=\omega_s)} - L(\partial \tilde{h}/\partial \omega_{(\omega=\omega_s)})$, where ω_s is the operating steady state, lie in the open left half of the complex plane. The state observer of Eq. 23 consists of a replica of the system of Eq. 10 plus a linear gain multiplying the discrepancy between the actual and the estimated value of the output, and, therefore, it is an extended Luenberger-type observer. Finally, the state feedback control law of Eq. 22 and the state observer of Eq. 23 can be combined to yield the desired bounded nonlinear output feedback control law.

We are now is a position to state the main result of this subsection. Theorem 1 below provides the explicit synthesis formula for the desired bounded output feedback control law and states precise conditions that guarantee closed-loop stability and asymptotic output tracking in the presence of input constraints in the closed-loop ODE system (the proof can be found in the appendix).

Theorem 1. Consider the system of Eq. 10 and assume that: (1) it is locally observable in the sense that there exists a matrix L such that $C_L = (1/\mu)\,\bar{A}$ where μ is a small positive parameter and $\bar{A}$ where $\bar{A}$ is a Hurwitz matrix; (2) its characteristic matrix, $C(\tilde{x})$, is nonsingular $\forall \tilde{x} \in D \subset \mathbb{R}^{n+N}$; (3) its inverse dynamics are input-to-state stable and exponentially stable when $\zeta = 0$. Consider first the system of Eq. 10 under the state feedback controller of Eq. 22 where

$$\frac{1}{2} R^{-1}(\tilde{x}) = \frac{L_{\tilde{f}}^* V + \sqrt{\left(L_{\tilde{f}}^* V\right)^2 + \left(u_{\max}^2 \left(L_{\tilde{g}} V\right)\left(L_{\tilde{g}} V\right)^T\right)^2}}{\left(L_{\tilde{g}} V\right)\left(L_{\tilde{g}} V\right)^T \left[1 + \sqrt{1 + u_{\max}^2 \left(L_{\tilde{g}} V\right)\left(L_{\tilde{g}} V\right)^T}\right]} \tag{24}$$

and $L_{\tilde{f}}^* V = L_{\tilde{f}} V + \rho |e|^2$, $\rho > 0$. Let δ_x be a positive real number such that the compact set $|\tilde{x}| \le \delta_x$ is the largest invariant set embedded within the unbounded region described by the following inequality

$$L_{\tilde{f}}^* V \le u_{\max} \left| \left(L_{\tilde{g}} V\right)^T \right| \tag{25}$$

Then, for any initial condition that satisfies $|\tilde{x}(0)| \le \delta_x$, the closed-loop system under state feedback control is asymptotically stable in the sense that there exists a function β of class KL such that $|x(t)| \le \beta(|x(0)|, t)$, $\forall t \ge 0$. Now consider the system of Eq. 10 under the output feedback controller

$$\frac{d\omega}{dt} = \tilde{f}(\omega) - \frac{1}{2}\tilde{g}(\omega) R^{-1}(\omega)\left[L_{\tilde{g}} V(\omega)\right]^T + L\left[y - \tilde{h}(\omega)\right]$$

$$u = -\frac{1}{2} R^{-1}(\omega)\left[L_{\tilde{g}} V(\omega)\right]^T \tag{26}$$

Then given any pair of positive real numbers (d, δ_b) such that $\beta(\delta_b, 0) + d \le \delta_x$, there exists $\mu^* > 0$ such that, if $\mu \in (0, \mu^*]$, $|\tilde{x}(0)| \le \delta_b$, $|\omega(0)| \le \delta_b$, the following holds in the presence of input constraints: (1) the closed-loop system is asymptotically (and locally exponentially) stable; (2) the output of the closed-loop ODE system satisfies a relation of the form $\lim_{t \to \infty} |y_{si} - v_i| = 0$, where v_i is the set point for the ith controlled output.

Remark 5. Theorem 1 provides an explicit characterization of a set of admissible initial conditions starting from where the constrained closed-loop ODE system is guaranteed to be stable with the available control action (region of guaranteed closed-loop stability). This characterization can be obtained from the inequality of Eq. 25. This inequality describes the largest region in state space where $\dot{V}$ is negative definite under the bounded state feedback controller of Eqs. 22–24 and where any closed-loop trajectory evolving is guaranteed to converge to the desired equilibrium point with the available control action. However, since this region is, in general, not an invariant one, it is necessary to guarantee that trajectories starting within the region do not leave, in order to guarantee closed-loop stability. This is done by confining the initial conditions within the largest invariant set embedded within the region. The size of this set is fixed by δ_x and represents the state feedback estimate of the region of closed-loop stability (see El-Farra and Christofides (2001a) and chapter 4 in Khalil (1996) for how to compute this estimate). According to Theorem 1, this estimate remains practically preserved under output feedback. Specifically, starting from any compact subset (whose size is fixed by δ_b) of the state feedback region, there always exists $\mu > 0$ such that the desired closed-loop properties are guaranteed under the dynamic *output* feedback controller of Eq. 26. Note that the size of the output feedback region (δ_b) can be made close to that of the state feedback region (δ_x) by selecting d to be sufficiently small which, in turn, can be done by choosing μ to be sufficiently small. Therefore, although combination of

the bounded state feedback controller with an observer results in some loss (represented by d) in the size of the region of guaranteed closed-loop stability, this loss can be made small by selecting μ to be sufficiently small.

Remark 6. The inequality of Eq. 25 captures, in an intuitive way, the dependence of the size of the region of guaranteed closed-loop stability on the magnitude of input constraints. For example, this inequality predicts that the tighter the input constraints are made (that is, smaller $u_{\max}$), the smaller the resulting closed-loop stability region. This is consistent with one's intuition, since under tight constraints, only few initial conditions are admissible and can be used to stabilize the closed-loop system. Finally, note that, according to the inequality of Eq. 25, the largest region of closed-loop stability under the control law of Eq. 22 is obtained, as expected, in the absence of constraints (that is, as $u_{\max} \to \infty$).

Remark 7. Note that the static feedback component of the proposed output feedback controller of Eq. 26 (with $\omega = \tilde{x}$) directly uses the available information on input constraints to achieve the requested closed-loop stability and performance properties (note the explicit dependence of the expression in Eq. 24 on $u_{\max}$). Note also that, whenever Eq. 25 holds, the control action is bounded by $u_{\max}$ and satisfies the constraints. Both the explicit incorporation of constraints in the controller design and the explicit characterization of the region of guaranteed closed-loop stability follow directly from inherent boundedness property of the state feedback component in Eq. 26. The state feedback component of Eqs. 22–24 involves a modification of the controller design proposed by Lin and Sontag (1991) by introducing $-\rho/e/^2$ which ensures that the constrained finite-dimensional closed-loop system is locally exponentially stable.

Remark 8. The bounded nonlinear controller of Eq. 22 possesses certain optimality properties characteristic of its ability to use small control action to accomplish the desired closed-loop objectives. In fact, one can rigorously prove, through the inverse optimal control approach (Freeman and Kokotovic, 1996; Sepulchre et al., 1997; El-Farra and Christofides, 2001a), that within a well-defined region of the closed-loop stability region, this controller is optimal with respect to an infinite-time meaningful quadratic cost functional of the form

$$J = \int_0^\infty \left[e^T Q(\tilde{x}) e + u^T R(\tilde{x}) u \right] dt \tag{27}$$

which imposes penalty on both the tracking error and control action. In the prior performance index, $Q(\tilde{x})$ is a positive definite matrix that can be found directly from the steady-state Hamilton-Jacobi-Bellman (HJB) equation (which is the optimality condition for the stabilization problem) associated with the system of Eq. 10 and cost functional of Eq. 27

$$0 \equiv e^T Q(\tilde{x}) e + L_{\tilde{f}} V - \frac{1}{4} \left(L_{\tilde{g}} V \right) R^{-1}(\tilde{x}) \left(L_{\tilde{g}} V \right)^T \tag{28}$$

The inverse optimal approach provides a rigorous framework for associating meaningful optimality (that is, meaningful performance indices) with certain stabilizing controllers (such as those of Eq. 22) and therefore helps explain the basis for their optimality properties. The key idea of this approach is to first design a stabilizing controller and then show that it minimizes a meaningful performance index of the form of Eq. 27 by establishing that the resulting weights Q, R are positive definite, which, in turn, renders the penalties imposed in the cost functional sensible. This approach has been used in the literature for the design of nonlinear optimal controllers without recourse to the unwieldy task of solving the HJB equation. For additional details on controller design using this approach, as well as some of the history and motivation behind it, refer to Sepulchre et al. (1997), and El-Farra and Christofides (2001a). Finally, one can easily show that the minimum cost achieved by the state feedback controller is $V[e(0)]$.

Remark 9. The controller-observer combination of Eq. 26 practically preserves the optimality properties of the state feedback controller explained in the previous remark. The output feedback controller design is near-optimal in the sense that the cost incurred by implementing this controller on the system of Eq. 10 tends to the optimal (minimal) cost achieved by implementing the bounded optimal state feedback controller (that is, u of Eq. 26 with $\omega = \tilde{x}$) when μ is selected to be sufficiently small. Using a standard singular perturbation argument, one can show that cost associated with the output feedback controller is $O(\mu)$ close to that optimal cost associated with the state feedback controller (that is, $J_{\min} = V(e(0)) + O(\mu)$). The basic reason for near-optimality is the fact that by choosing μ to be sufficiently small, the observer states can be made to converge quickly to the process states. This fact can be exploited to make the performance of the output feedback controller arbitrarily close to that of the optimal state feedback controller.

Remark 10. The requirement that the observer states start within the region of guaranteed closed-loop stability ($|\omega(0)| \leq \delta_b$) is motivated by the fact that the process states themselves should start inside this region in order to guarantee stability of the constrained closed-loop system and, therefore, one must initiate the observer within the same region to guarantee convergence of the observer states to the process states. Note, however, that no restriction is placed on where, inside the stability region, the observer states can start (that is, we allow for initialization errors) since they can be made to converge sufficiently fast to the actual states by selecting μ to be sufficiently small.

Remark 11. Regarding the practical application of Theorem 1, one has to initially use the method of weighted residuals to derive an ODE system of the form of Eq. 10, and then verify assumptions 1, 2 and 3 on the basis of this system. Then, given the available input constraints $u_{\max}$ and the desired initial condition, one should check if the inequality of Eq. 25 is satisfied and if the initial condition lies within the region of guaranteed closed-loop stability. If this is the case, then the desired closed-loop properties are guaranteed and the synthesis formula of Eq. 26 can be directly used to derive the explicit form of the controller and implement it.

Application to the crystallizer moment model

The objective of the subsection is to illustrate an application of the results of Theorem 1 to the fifth-order moment model of Eq. 14 which describes the dominant dynamics of the continuous crystallizer of Eq. 4. In particular, we demon-

strate the ability of the bounded nonlinear controller to handle input constraints by identifying explicitly the initial conditions that guarantee stability of the constrained closed-loop system. The control problem here is the same as that considered in the motivating example which involves regulating the crystal concentration by manipulating the solute feed concentration in the presence of constraints on the manipulated input. Utilizing the dimensionless variables of Eq. 15, the system of Eq. 14 can be recast in the form of Eq. 10 with $\tilde{x} = [\tilde{x}_0\ \tilde{x}_1\ \tilde{x}_2\ \tilde{x}_3\ \tilde{y}]^T$ and

$$\tilde{f}(\tilde{x}) = \begin{bmatrix} -\tilde{x}_0 + (1-\tilde{x}_3)\,Dae^{\frac{-F}{\tilde{y}^2}} \\ -\tilde{x}_1 + \tilde{y}\tilde{x}_0 \\ -\tilde{x}_2 + \tilde{y}\tilde{x}_1 \\ -\tilde{x}_3 + \tilde{y}\tilde{x}_2 \\ \dfrac{1-\tilde{y}-(\alpha-\tilde{y})\tilde{y}\tilde{x}_2}{1-\tilde{x}_3} \end{bmatrix}, \quad \tilde{g}(\tilde{x}) = \begin{bmatrix} 0 \\ 0 \\ 0 \\ 0 \\ 1 \\ \hline 1-\tilde{x}_3 \end{bmatrix}$$

On the basis of this system, one can easily verify that assumptions 1, 2 and 3 of Theorem 1 are satisfied. Assumption 3 in particular can be verified, in principle, using a standard Lyapunov argument applied to the inverse dynamics of the system. For the specific example under consideration, it is relatively straightforward to obtain explicit analytical expressions for the inverse dynamics of the fifth-order moment model by performing a standard nonlinear transformation of the type given in Eq. 18. The inverse dynamics for this specific system have a simple structure that can be easily exploited to show nonlocal stability. In fact, the zero dynamics have the form $\dot{\eta}_i = -\eta_i$, $i = 1, 2, 3$, which is globally exponentially stable. A direct application of the synthesis formula of Eq. 26 then yields the following bounded nonlinear output feedback controller

$$\begin{aligned}
\dot{\omega}_0 &= -\omega_0 + (1-\omega_3)\,Dae^{\frac{-F}{\omega_4^2}} + L_0[\tilde{x}_0 - \omega_0] \\
\dot{\omega}_1 &= -\omega_1 + \omega_4\omega_0 + L_1[\tilde{x}_0 - \omega_0] \\
\dot{\omega}_2 &= -\omega_2 + \omega_4\omega_1 + L_2[\tilde{x}_0 - \omega_0] \\
\dot{\omega}_3 &= -\omega_3 + \omega_4\omega_2 + L_3[\tilde{x}_0 - \omega_0] \\
\dot{\omega}_4 &= \frac{1-\omega_4-(\alpha-\omega_4)\omega_4\omega_2}{1-\omega_3} \\
&\quad -\frac{1}{2}\frac{R^{-1}(\omega)L_{\tilde{g}}V(\omega)}{1-\omega_3} + L_4[\tilde{x}_0 - \omega_0] \\
u &= -\frac{1}{2}R^{-1}(\omega)L_{\tilde{g}}V(\omega)
\end{aligned} \tag{29}$$

where

$$V = e^T P e, \quad P = \begin{bmatrix} 1 & c' \\ c' & 1 \end{bmatrix}, \quad c' \in (0,1) \tag{30}$$

Guided by the information in Figure 3, we constrain the manipulated input in the interval $[0, 6]$ so that the requested set point of $\tilde{x}_0 = 0.4$ is an admissible one. Two closed-loop simulation runs, starting from two different initial conditions, were performed to evaluate the set point tracking capability of the bounded nonlinear output feedback controller of Eq. 29 in the presence of constraints. The initial conditions for the states of the moment model, the states of the observer, and the values of the nonlinear controller parameters are all given in Table 2 for both runs. Note that in both cases, the initial observer states do not match those of the moment model to study the performance of the controller in the presence of initialization errors.

Table 2. Initial Conditions and Tuning Parameters for Bounded Nonlinear Controller Using Crystallizer Moment Model

	First Run	Second Run
$\tilde{x}(0)$	$[0.059\ 0.035\ 0.022\ 0.014\ 0.60]^T$	$[0.44\ 0.61\ 0.85\ 1.14\ 0.60]^T$
$\omega(0)$	$[0.047\ 0.028\ 0.017\ 0.010\ 0.60]^T$	$[0.42\ 0.59\ 0.80\ 1.07\ 0.60]^T$
L	$[1.0\ 0.0\ 0.0\ 0.0\ 1.0]^T$	$[1.0\ 0.0\ 0.0\ 0.0\ 1.0]^T$
c'	0.90	0.90
ρ	0.001	0.001

The first simulation run considered stabilizing the crystallizer at the setpoint of $\tilde{x}_0 = 0.4$ starting from an initial condition that belongs to the region of guaranteed closed-loop stability (from the inequality of Eq. 25). Figure 4 shows the closed-loop output (top plot) and manipulated input (bottom plot) profiles for this case. It clearly shows that, starting from this initial condition, the bounded output feedback controller successfully achieves the requested setpoint and generates

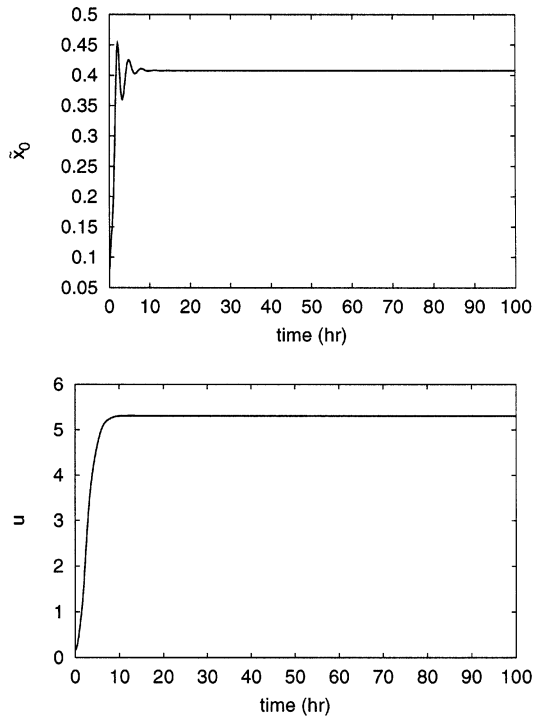

Figure 4. Controlled output (crystal concentration) and manipulated input (solute concentration) for crystallizer moment model under bounded nonlinear controller with constrained process input in [0, 6] and initial condition inside closed-loop stability region.

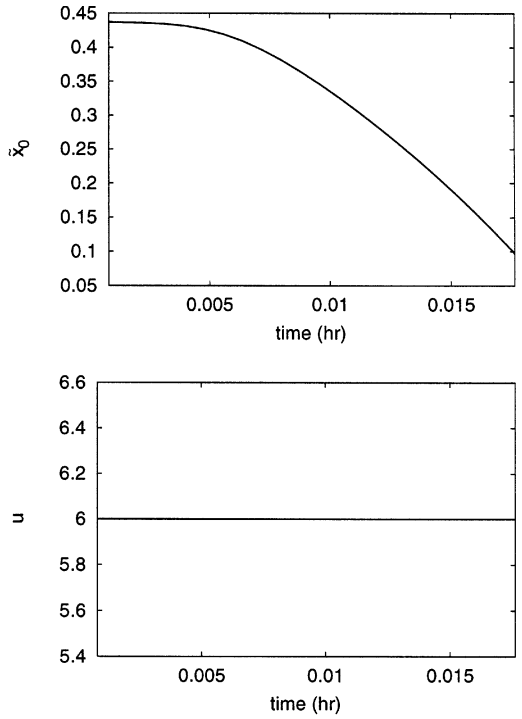

Figure 5. Controlled output (crystal concentration) and manipulated input (solute concentration) for crystallizer moment under bounded nonlinear controller with constrained process input [0, 6], and initial condition that violates Eq. 25.

control action that satisfies the process input constraints. The second simulation run considered the same setpoint starting from an initial condition that lies outside the region of guaranteed closed-loop stability (the initial condition for the second run in Table 2 does not satisfy Eq. 25). The closed-loop output and manipulated input profiles for this run (Figure 5) show that in this case the controller is unable to achieve the requested setpoint in the presence of constraints although the requested setpoint is admissible.

The underlying cause for the instability in Figure 5 is the fact that the initial condition lies outside the region of closed-loop stability, and, therefore, the control action required to drive that initial condition to the desired set point is larger than that available due to the constraints (compare with Figure 4). This leads to the process input being saturated for all times as the controller tries unsuccessfully to provide the maximum solute feed concentration to achieve the desired crystal concentration. Note that based on the stability analysis of Theorem 1, we can conclude that there is no guarantee that a set point of $\tilde{x}_0 = 0.4$ can be reached from the given initial condition (which is the only thing of practical concern), but cannot predict how the state $\tilde{x}_0$, once unstable, will evolve. Therefore, to explain the runaway behavior in Figure 5, we may view the closed-loop system under fixed input (see the input profile in Figure 5) as an open-loop system and analyze the stability properties of its equilibrium point. Under a fixed input of $u = 6$, this system has an unstable equilibrium point at $\tilde{x}_0 = 0.45$ (note that this is not the desired set point). Therefore, once under a fixed input of $u = 6$, the state $\tilde{x}_0$ does not stabilize at 0.45 and runs away instead. Had this equilibrium point been a stable one, the state $\tilde{x}_0$ would have settled there. However, this is not the desired set point. So, regardless of this equilibrium point's stability or instability, the controller is unable to achieve the desired set point of $\tilde{x}_0 = 0.4$. Note that this reasoning, based on open-loop stability analysis, explains only why the state $\tilde{x}_0$, once under fixed input, runs away instead of settling at another steady state (that is, it explains the type of instability that occurs), but does not explain why the process input remains fixed in the first place which is the underlying cause of instability. The answer to this question is provided by Theorem 1 and has to do with the selection of an inadmissible initial condition.

Controller implementation on the infinite-dimensional particulate process model

Based on the ODE system of Eq. 10, we have designed a bounded nonlinear output feedback controller with well characterized stability properties in the presence of constraints and illustrated its application to the constrained low-dimensional ODE system of Eq. 10 which captures the dominant dynamics of the particulate process. Now, we proceed with the final step of our methodology and implement the bounded output feedback controller of Eq. 26 on the infinite dimensional particulate process model of Eq. 1. Theorem 2 states precise conditions that guarantee closed-loop stability and asymptotic output tracking in the presence of constraints. The proof of this theorem is in the appendix.

Theorem 2. Consider the system of Eq. 10, for which assumptions 1, 2, and 3 of Theorem 1 hold. Consider also the particulate process model of Eq. 1 under the nonlinear output feedback controller of Eq. 26. Then, for sufficiently large N, there exist positive real numbers, δ_n, $\bar{\delta}_x$, δ_w, $\bar{\mu}^*$ *such that if* $\mu \in (0, \bar{\mu}^*]$, $\| n(r,0) \|_2 < \delta_n$, $|x(0)| < \bar{\delta}_x$, $|\omega(0)| < \delta_w$*: (1) The closed-loop system (particulate process model and controller of Eq. 26) is exponentially stable. (2)* $\lim_{t \to \infty} |y_i - v_i| = O(\epsilon(N))$*, where* v_i *is the set point for the ith controlled output and* $\epsilon(N)$ *is a small positive real number that depends on N and satisfies* $\lim_{N \to \infty} \epsilon(N) = 0$.

Remark 12. Theorem 2 establishes that a bounded nonlinear output feedback controller, which guarantees exponential stability and output tracking in the constrained finite-dimensional closed-loop system (Eqs. 10–26), continues to enforce the same properties locally in the constrained infinite-dimensional closed-loop system (Eqs. 1–26). This result is intuitively expected, because for sufficiently large N: (a) the dynamics of the modes of the particulate process model which are not taken into account in the controller design (that is, not included in the ODE model of Eq. 10) are locally exponentially stable, and (b) the control action $u(t)$ does not influence the dynamics of the modes which are not taken into account in the controller design.

Remark 13. It was pointed out in Remark 5 that the inequality of Eq. 25 provides an estimate of the set of admissible initial conditions starting from where the constrained finite-dimensional closed-loop system (Eqs. 10–26) is guaran-

teed to be stable. Note that owing to the infinite-dimensional nature of the particulate process model of Eq. 1, this inequality cannot be used directly to check the admissible initial conditions of the infinite-dimensional system (this is, because the amplitude of the residual modes not included in the controller design may not, in general, be negligible). Furthermore, the local nature of the result of Theorem 2 implies that the initial conditions, for the infinite-dimensional system, must be selected sufficiently small to guarantee exponential stability of the closed-loop system. However, the inequality of Eq. 25 continues to provide a useful guide for the selection of the admissible initial observer states that guarantee stability of the constrained infinite-dimensional closed-loop system (Eqs. 1–26). To see why this is the case, recall from Theorem 1 that the selection of the initial observer states within the largest invariant subset of the region described by Eq. 25 guarantees stability of the constrained finite-dimensional closed-loop system (and, consequently, local exponential stability of the infinite-dimensional system according to Theorem 2). Guided by this result, we conclude that, in order to guarantee stability of the constrained infinite-dimensional closed-loop system, the initial observer states should, at a minimum, not be chosen outside this region. The region of Eq. 25 therefore provides a reasonable initial guess for where to initialize the observer.

Application to a Continuous Crystallizer with Input Constraints

The proposed nonlinear control method is used in this section to stabilize the continuous crystallizer, introduced earlier, in the presence of input constraints. Motivated by the fact that the crystallizer with the crystal-size distribution as controlled output, and the solute feed concentration as manipulated input, is an approximately controllable system (see Semino and Ray (1995a) for a rigorous controllability analysis), we consider the control problem of manipulating the solute feed concentration to achieve a crystal-size distribution with desired mass. Refer to Randolph et al. (1987), Eaton and Rawlings (1990), and Rawlings et al. (1993) for the use of other manipulated variables including fines destruction rate and crystallizer temperature for the stabilization of crystallizers (note that the proposed control method can be used for the synthesis of nonlinear controllers when such manipulated inputs are considered).

Following the methodology already outlined, the design of the necessary bounded nonlinear output feedback controller is carried out on the basis of the low-dimensional ODE model (moment model) of Eq. 14 which captures the dominant dynamics of the crystallizer. The controller design procedure, as well as the explicit controller formula, were given in the previous section where the controller was first implemented on the constrained ODE model. Here we implement the same controller on the constrained infinite-dimensional crystallizer model of Eq. 4. The practical implementation of the nonlinear controllers of Eq. 29 requires online measurements of the controlled output, $\tilde{x}_0$; in practice, such measurements can be obtained by using, for example, light scattering (Bohren and Huffman, 1983; Rawlings et al., 1993).

Several simulation runs were performed to evaluate the performance, robustness, and constraint-handling properties of the bounded nonlinear controller of Eq. 29, and compare them with those of a PI controller. The values of the nonlinear controller parameters and the PI controller parameters K_c, τ_I, which were used in the simulations, are given in Table 3 (K_c, τ_{I} were computed through extensive trial and error). In all the simulation runs, the initial condition

$$n(r,0) = 0.0,\ c(0) = 990.0\ \mathrm{kg/m^3}$$

was used for the process model of Eq. 4 and the finite difference method with 1,000 discretization points was used for its simulation. The initial conditions for the dynamic system included in the controller of Eq. 29 were set to be: $\omega_0 = 0.047$, $\omega_1 = 0.028$, $\omega_2 = 0.017$, $\omega_3 = 0.01$ and $\omega_4 = 0.5996$ (note that they do not correspond to the initial conditions used for the distributed parameter model in order to study the performance of the controller in the presence of significant initialization errors).

Table 3. Tuning Parameters for PI and Bounded Nonlinear Controller Using Infinite-Dimensional Crystallizer Model

	Nominal Conditions	Parametric Uncertainty
K_c	0.5	0.5
τ_I	1.5	1.0
$'_c$	0.90	0.90
ρ	0.001	0.001
τ_i'	—	1.0

In the first set of simulation runs, the set point tracking capability of the nonlinear controller in the presence of input constraints ($u \in [0,6]$) was evaluated under nominal conditions for a 0.4 increase in the value of the set point ($\upsilon = 0.4$). Figure 6 shows the closed-loop output (top plot) and manipulated input (middle plot) profiles obtained by using the bounded nonlinear controller (solid lines) of Eq. 29. For the sake of comparison, the corresponding profiles under PI control are also included (dashed lines). Clearly, the bounded nonlinear controller drives the controlled output to its new set point value in a significantly shorter time than the one required by the PI controller (note that the controlled output under the nonlinear controller exhibits smaller overshoot). Note also the superior transient behavior of the closed-loop output under the bounded nonlinear controller compared to the oscillatory response obtained under PI control. Any further retuning of the PI controller leads to an unreasonably large overshoot in the controlled output. For the same simulation run, the evolution of the closed-loop profile of the crystal-size distribution is shown in Figure 6 (bottom plot). An exponentially-decaying crystal-size distribution is obtained at the steady state.

Next, the robustness properties of the bounded nonlinear controller in the presence of parametric uncertainties were investigated, for a 0.4 increase in the value of the set point. To ensure offsetless tracking in the presence of constant uncertainty in process parameters, the bounded nonlinear controller of Eq. 29 was complemented with integral action (that is, the term $\upsilon - \tilde{h}(\omega)$ was substituted by $\upsilon - y + (1/\tau_i')\xi$, where $\dot{\xi} = \upsilon - y$, $\xi(0) = 0$ and τ_i' is the integral time constant). Figure 7 shows the closed-loop output (top plot), ma-

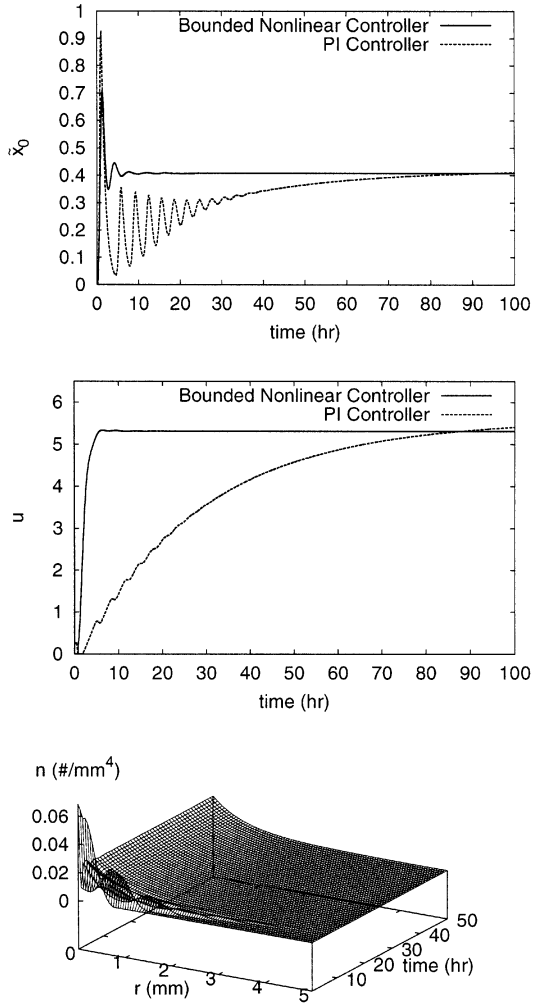

Figure 6. Controlled output (crystal concentration), manipulated input (solute concentration), and crystal-size distribution for crystallizer process model of Eq. 4 under bounded nonlinear controller (solid line) and PI controller (dashed line) for 0.4 increase in the set point and $u \in [0,6]$.

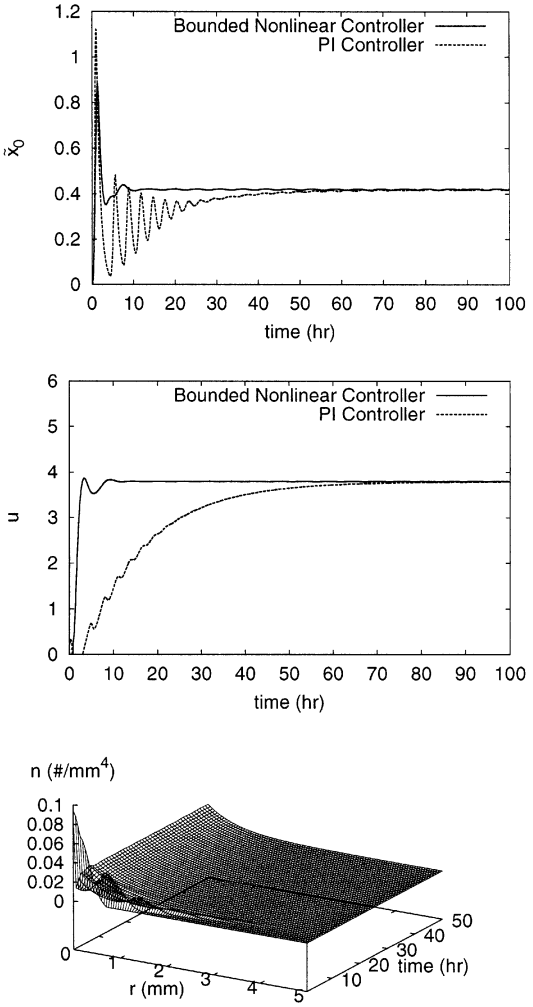

Figure 7. Controlled output (crystal concentration), manipulated input (solute concentration), and crystal-size distribution for crystallizer process model of Eq. 4 under bounded nonlinear controller (solid line) and PI controller (dashed line) for 0.4 increase in the set point with input constraints $u \in [0,6]$ and 5% modeling error in both F and τ.

nipulated input (middle plot), and evolution of the crystal-size distribution (bottom plot) profiles under the bounded nonlinear controller (solid lines) in the presence of 5% error in both F and τ. The corresponding output and input profiles under PI control are also included (dashed lines). We observe that the bounded nonlinear controller exhibits very good robustness properties, driving the output quickly to its new set point.

Finally, we tested the robustness of the bounded nonlinear controller in the presence of unmodeled actuator and sensor dynamics. To account for the actuator and sensor dynamics, the process model of Eq. 4 was augmented with the dynamical system $\epsilon_a \dot{z}_1 = -z_1 + z_2$, $\epsilon_a \dot{z}_2 = -z_2 + u$ and the dynamical system $\epsilon_s \dot{z}_3 = -z_3 + z_4$, $\epsilon_s \dot{z}_4 = -z_4 + y$, where $z_1, z_2 \in \mathbb{R}$ are the actuator states, $z_3, z_4 \in \mathbb{R}$ are the sensor states, z_1 is the actuator output, z_3 is the sensor output, and ϵ_a, ϵ_s are small parameters characterizing how fast the actuator and sensor dynamics are, respectively. In this case, the bounded nonlinear controller was also found to be robust with respect to unmodeled dynamics for $\epsilon_a = \epsilon_s = 0.05$. The corresponding closed-loop output (top plot), manipulated input (middle plot), and evolution of crystal-size distribution (bottom plot) profiles are depicted in Figure 8.

Conclusions

In this work, we considered spatially-homogeneous particulate processes with input constraints and developed a rigorous and general methodology for the analysis and control of such processes. Initially, a model reduction procedure based on the method of weighted residuals was presented for the construction of finite-dimensional ODE systems that accurately reproduce the dynamics of the particulate process. These ODE systems were then used to identify the set of feasible control objectives (set points) that can be achieved in the presence of constraints. This information together with

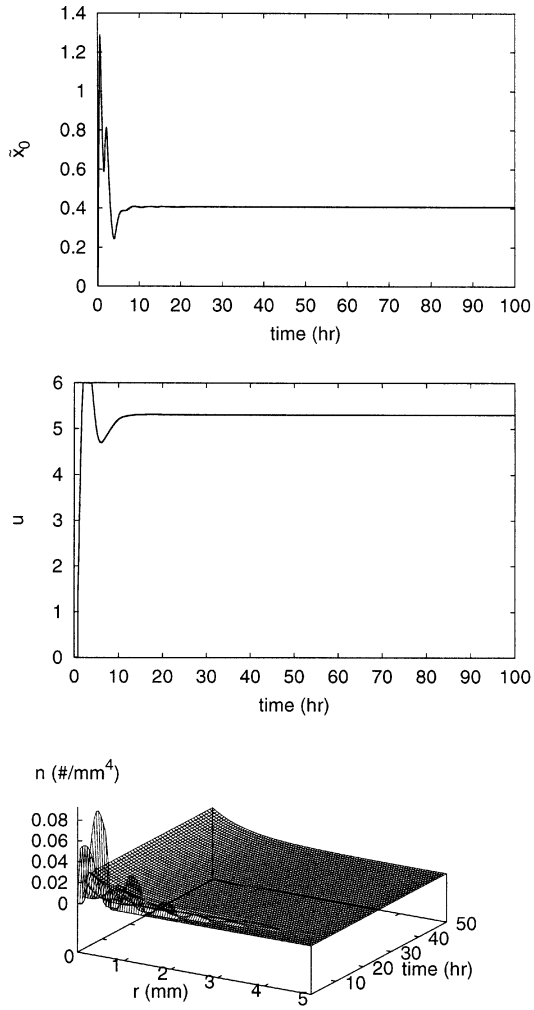

Figure 8. Controlled output (crystal concentration), manipulated input (solute concentration), and crystal-size distribution for crystallizer process model of Eq. 4 under bounded nonlinear controller for 0.4 increase in the set point with input constraints $u \in [0, 6]$ and actuator and sensor unmodeled dynamics.

the derived ODE systems was then used as the basis for the synthesis of practically-implementable nonlinear bounded output feedback controllers that enforce exponential stability in the closed-loop system and achieve particle-size distributions with desired characteristics, in the presence of active input constraints. Precise closed loop stability conditions were given and controller implementation issues were addressed. The proposed methodology was successfully applied to a continuous crystallizer, which exhibits open-loop unstable (oscillatory) behavior, and shown to cope effectively with the problem of constraints.

Acknowledgment

Financial support from a National Science Foundation CAREER award, CTS 9533509 and the Office of Naval Research (2001 Young Investigator Award) is gratefully acknowledged.

Literature Cited

Alvarez, J., J. J. Alvarez, and R. Suarez, "Nonlinear Bounded Control for a Class of Continuous Agitated Tank Reactors," *Chem. Eng. Sci.*, **46**, 3235 (1991).

Bohren, C. F., and D. R. Huffman, *Absorption and Scattering of Light by Small Particles*, Wiley, New York (1983).

Chiu, T., and P. Christofides, "Nonlinear Control of Particulate Processes," *AIChE J.*, **45**, 1279 (1999).

Chiu, T., and P. Christofides, "Robust Control of Particulate Processes Using Uncertain Population Balances," *AIChE J.*, **46**, 266 (2000).

Chmieleweski, D., and V. Manousiouthakis, "Constrained Infinite-Time Nonlinear Quadratic-Optimal Control with Application to Chemical Reactors," *Proc. of Conf. on Control Applications*, Honolulu, HI (1998).

Christofides, P. D., and A. R. Teel, "Singular Perturbations and Input-to-State Stability," *IEEE Trans. Autom. Contr.*, **41**, 1645 (1996).

Colonius, F., and W. Kliemann, "Some Aspects of Control of Systems as Dynamical Systems," *J. Dynamics and Differential Equations*, **5**, 469 (1993).

Dimitratos, J., G. Elicabe, and C. Georgakis, "Control of Emulsion Polymerization Reactors," *AIChE J.*, **40**, 1993 (1994).

Eaton, J. W., and J. B. Rawlings, "Feedback Control of Chemical Processes Using On-Line Optimization Techniques," *Comp. Chem. Eng.*, **14**, 469 (1990).

El-Farra, N. H., and P. D. Christofides, "Integrating Robustness, Optimality, and Constraints in Control of Nonlinear Processes," *Chem. Eng. Sci.*, **56** (2001a).

El-Farra, N. H., and P. D. Christofides, "Robust Near-Optimal Output Feedback Control of Nonlinear Systems," *Intr. J. Contr.*, **74**, 133 (2001b).

Fisher, W. R., M. F. Doherty, and J. M. Douglas, "Steady-State Control as a Prelude to Dynamic Control, " *Chem. Eng. Res. Des.*, **6**, 353 (1985).

Freeman, R. A., and P. V. Kokotovic, *Robust Nonlinear Control Design: State-Space and Lyapunov Techniques*, Birkhauser, Boston (1996).

Friedlander, S. K., *Smoke, Dust, and Haze: Fundamentals of Aerosol Behavior*, Wiley, New York (1977).

Gelbard, F., and J. H. Seinfeld, "Numerical Solution of the Dynamic Equation for Particulate Processes," *J. Comp. Phys.*, **28**, 357 (1978).

Hill, P. J., and K. M. Ng, "New Discretization Procedure for the Agglomeration Equation," *AIChE J.*, **42**, 727 (1996).

Jerauld, G. R., Y. Vasatis, and M. F. Doherty, "Simple Conditions for the Appearance of Sustained Oscillations in Continuous Crystallizers," *Chem. Eng. Sci.*, **38**, 1675 (1983).

Kapoor, N., and P. Daoutidis, "On the Dynamics of Nonlinear Systems with Input Constraints," *Chaos*, **9**, 88 (1999).

Khalil, H. K., *Nonlinear Systems*, 2nd ed., Macmillan, New York (1996).

Kothare, M. V., P. J. Campo, M. Morari, and C. N. Nett, "A Unified Framework for the Study of Anti-Windup Designs," *Automatica*, **30**, 1869 (1994).

Kumar, S., and D. Ramkrishna, "On the Solution of Population Balance Equations by Discretization—I. A Fixed Pivot Technique," *Chem. Eng. Sci.*, **51**, 1311 (1996a).

Kumar, S., and D. Ramkrishna, "On the Solution of Population Balance Equations by Discretization-II. a Moving Pivot Technique," *Chem. Eng. Sci.*, **51**, 1333 (1996b).

Kurtz, M. J., G.-Y. Zhu, A. Zamamiri, M. A. Henson, and M. A. Hjortso, "Control of Oscillating Microbial Cultures Described by Population Balance Models," *Ind. Eng. Chem. Res.*, **37**, 4059 (1998).

Lin, Y., and E. D. Sontag, "A Universal Formula for Stabilization with Bounded Controls," *Systems & Control Lett.*, **16**, 393 (1991).

Nicmanis, M., and M. J. Hounslow, "Finite-Element Methods for Steady-State Population Balance Equations," *AIChE J.*, **44**, 2258 (1998).

Oliveira, S. L., V. Nevistic, and M. Morari, "Control of Nonlinear Systems Subject to Input Constraints," *Proc. of Symp. on Nonlinear Control Systems Design '95*, p. 913, Tahoe City, CA (1995).

Ramkrishna, D., "The Status of Population Balances," *Rev. Chem. Eng.*, **3**, 49 (1985).

Randolph, A. D., L. Chen, and A. Tavana, "Feedback Control of

CSD in a KCl Crystallizer with a Fines Dissolver, *AIChE J.*, **33**, 583 (1987).
Rawlings, J. B., "Tutorial: Model Predictive Control Technology," *Proc. of Amer. Control Conf.*, San Diego, CA, p. 662 (1999).
Rawlings, J. B., S. M. Miller, and W. R. Witkowski, "Model Identification and Control of Solution Crystallization Processes," *I&EC Res*., **32**, 1275 (1993).
Rawlings, J. B., and W. H. Ray, "Stability of Continuous Emulsion Polymerization Reactors: A Detailed Model Analysis," *Chem. Eng. Sci.*, **42**, 2767 (1987).
Rohani, S., and J. R. Bourne, "Self-Tuning Control of Crystal Size Distribution in a Cooling Batch Crystallizer," *Chem. Eng. Sci.*, **12**, 3457 (1990).
Schwarm, A. T., and M. Nikolaou, "Chance-Constrained Model Predictive Control," *AIChE J.*, **45**, 1743 (1999).
Semino, D., and W. H. Ray, "Control of Systems Described by Population Balance Equations—I. Controllability Analysis," *Chem. Eng. Sci.*, **50**, 1805 (1995a).
Semino, D., and W. H. Ray, "Control of Systems Described by Population Balance Equations—II. Emulsion Polymerization with Constrained Control Action," *Chem. Eng. Sci.*, **50**, 1825 (1995b).
Sepulchre, R., M. Jankovic, and P. Kokotovic, *Constructive Nonlinear Control*, Springer-Verlag, Berlin-Heidelberg (1997).
Stephanopoulos, G., "Synthesis of Control Systems for Chemical Plants-A Challenge for Creativity," *Comp. & Chem. Eng*., **7**, 331 (1983).
Valluri, S., and M. Soroush, "Analytical Control of SISO Nonlinear Processes with Input Constraints," *AIChE J.*, **44**, 116 (1998).

Appendix

Proof of Theorem 1

Consider first the state feedback control problem. Substituting the controller of Eqs. 22–24 into Eq. 10 and transforming the resulting system into the form of Eqs. 18–19, the closed-loop system under state feedback can be written as

$$\begin{aligned}
\dot{e} &= Ae + B\Big\{l_1(e,\eta,\bar{v}) \\
&\qquad - \frac{1}{2}C(\tilde{x})R^{-1}(\tilde{x})\big[L_{\bar{g}}V(\tilde{x})\big]^T\Big\} \\
\dot{\eta}_1 &= \Psi_1(\zeta,\eta) \\
&\vdots \\
\dot{\eta}_{(n+N)-\Sigma_i r_i} &= \Psi_{(n+N)-\Sigma_i r_i}(\zeta,\eta) \\
y_{s_i} &= e_1^{(i)} + v_i, \quad i = 1, \ldots, m
\end{aligned} \tag{A1}$$

Consider the Lyapunov function candidate $V = e^T P e$ introduced in Theorem 1 and assume that the η states are bounded. Evaluating the time-derivative of this function along trajectories of the closed-loop e-subsystem in Eq. A1, we obtain

$$\begin{aligned}
\dot{V} &= L_{\bar{f}}V + L_{\bar{g}}Vu \\
&= \frac{-\rho|e|^2 + L_{\bar{f}}V\sqrt{1+u_{\max}^2\big(L_{\bar{g}}V\big)\big(L_{\bar{g}}V\big)^T} - \sqrt{\big(L_{\bar{f}}^*V\big)^2 + \Big(u_{\max}^2\big(L_{\bar{g}}V\big)\big(L_{\bar{g}}V\big)^T\Big)^2}}{\Big[1+\sqrt{1+u_{\max}^2\big(L_{\bar{g}}V\big)\big(L_{\bar{g}}V\big)^T}\Big]}
\end{aligned} \tag{A2}$$

It is clear from the above equation and from the fact that $\rho > 0$, that whenever $L_{\bar{f}}^*V \le 0$, we have $L_{\bar{f}}V \le 0$ and the time-derivative of V satisfies

$$\dot{V} \le \frac{-\rho|e|^2}{\Big[1+\sqrt{1+u_{\max}^2\big(L_{\bar{g}}V\big)\big(L_{\bar{g}}V\big)^T}\Big]} < 0 \ \forall e \neq 0 \tag{A3}$$

Furthermore, whenever $0 < L_{\bar{f}}^*V \le u_{\max}|(L_{\bar{g}}V)^T|$, we have

$$\begin{aligned}
&\sqrt{\big(L_{\bar{f}}^*V\big)^2 + \Big[u_{\max}^2\big(L_{\bar{g}}V\big)\big(L_{\bar{g}}V\big)^T\Big]^2} \\
&\qquad \ge L_{\bar{f}}V\sqrt{1+u_{\max}^2\big(L_{\bar{g}}V\big)\big(L_{\bar{g}}V\big)^T}
\end{aligned}$$

and $\dot{V}$ satisfies Eq. A3. Summarizing, whenever $L_{\bar{f}}^*V \le u_{\max}|(L_{\bar{g}}V)^T|$, the closed-loop e-subsystem is asymptotically stable. Since the η subsystem, with e as input, is ISS (from assumption 2), a standard small gain argument can be used to show that the closed-loop system of Eq. A1, under state feedback, is asymptotically stable whenever the inequality of Eq. 25 holds. To guarantee that this inequality holds for all time and that the closed-loop trajectories do not leave the unbounded regon described by Eq. 25 (hereafter denoted by Ω_1), we consider the largest invariant set (hereafter denoted by Ω_2) within Ω_1 and let δ_x denote the radius of Ω_2, that is, $\Omega_2 = \{\tilde{x} \in \mathbb{R}^{n+N} : |\tilde{x}| \le \delta_x\}$. Then, given any initial condition such that $|\tilde{x}(0)| \le \delta_x$, there exists a function β of class KL such that $|\tilde{x}(t)| \le \beta(|\tilde{x}(0)|, t)\ \forall t \ge 0$ and the state $\tilde{x}$ is bounded. Consequently, the denominator expression in Eq. A3 is bounded and there exists a positive real number k_1 such that $\dot{V} \le -k_1|e|^2$ and the closed-loop e-subsystem is exponentially stable and satisifies

$$|e(t)| \le K_e|e(0)|e^{-a_1 t}, \ \forall t \ge 0 \tag{A4}$$

for some $K_e \ge 1$, $a_1 > 0$.

Having established asymptotic stability under state feedback, we now consider the output feedback control problem. Substituting the output feedback controller of Eq. 26 into Eqs. 18–19, defining the observer error vector $e_o = \omega - \tilde{x}$ using the assumption $C_L = (1/\mu)\bar{A}$ where $\bar{A}$ is a Hurwitz matrix, and multiplying the $\dot{e}_o$-subsystem by μ, the closed-loop system can be written as

$$\mu\frac{de_o}{dt} = \bar{A}e_o + \mu\hat{f}(\omega, \tilde{x}, \upsilon)$$

$$\dot{e} = Ae + B\left[l_1(e, \eta, \bar{v}) - \frac{1}{2}C(\tilde{x})R^{-1}(\omega)\left(L_{\tilde{g}}V(\omega)\right)^T\right]$$

$$\dot{\eta}_1 = \Psi_1(\zeta, \eta)$$

$$\vdots$$

$$\dot{\eta}_{(n+N)-\sum_i r_i} = \Psi_{(n+N)-\sum_i r_i}(\zeta, \eta)$$

$$y_{s_i} = e_1^{(i)} + \upsilon_i, \quad i = 1, \ldots, m \tag{A5}$$

where $\hat{f}(\omega, \tilde{x}, \upsilon)$ is a nonlinear vector function whose explicit form is omitted for brevity. The above system is in a standard singularly perturbed form (Khalil, 1996) and possesses an exponentially stable fast subsystem: $de_o/d\tau = \bar{A}e_o$, where $\tau = t/\mu$, and a slow subsystem that has the exact same form as the system of Eq. A1 (closed-loop system under state feedback). We have already shown that this slow system is asymptotically stable for all initial conditions within Ω_2 and that its states are bounded. At this point, one can show, using calculations similar to those performed in Christofides and Teel (1996), that the bounds on the temporal evolution of the states of the closed-loop slow system (state feedback problem) continue to hold for the states of the closed-loop singularly pertubed system of Eq. A5 (output feedback problem), up to an arbitrarily small offset d, starting from initial conditions in arbitrarily large compact subsets (hereafter denoted by Ω_3) of Ω_2, where $\Omega_3 = \{\tilde{x} \in \mathbb{R}^{n+N}: |\tilde{x}| \le \delta_b\}$ and $\beta(\delta_b, 0) + d \le \delta_x$, provided that the singular perturbation parameter μ is sufficiently small. The requirement that $\beta(\delta_b, 0) + d \le \delta_x$ guarantees that the closed-loop trajectories remain within the invariant region Ω_2 for all time. Therefore, given the pair (δ_b, d), there exists $\mu' > 0$, such that if $\mu \le \mu'$, $|\tilde{x}(0)| \le \delta_b$, $|\omega(0)| \le \delta_b$, the states of the closed-loop system under output feedback are bounded. To establish asymptotic (and local exponential) stability, we note that the offset d can be made sufficiently small (by choosing μ sufficiently small), such that, after a sufficiently large time (when the exponential term in Eq. A4 dies out), the states of the closed-loop system are confined within a small neighborhood of the origin. Direct application then of the result of Theorem 9.3 in Khalil (1996) yields that there exists a μ^*, such that if $\mu \le \mu^*$, $|\tilde{x}(0)1| \le \delta_b$, $|\omega(0)1 \le \delta_b$, the closed-loop system of Eq. A5 is locally exponentially stable. Since the trajectories are bounded within Ω_3, then the closed-loop system is also asymptotically stable for all initial conditions within Ω_3. A somewhat similar argument was used in the proof of Theorem 1 in El-Farra and Christofides (2001b) (see this reference for mathematical details). The asymptotic output tracking result can be easily obtained by taking the limit of both sides of the inequality in Eq. A4 as $t \to \infty$ which yields $\lim_{t\to\infty} |e_1^{(i)}(t)| = \lim_{t\to\infty} |y_{si}(t) - \upsilon_i(t)| = 0$, $i = 1, \ldots, m$.

Proof of Theorem 2. Under the controller of Eq. 26, the infinite-dimensional closed-loop system takes the form

$$\frac{d\omega}{dt} = \tilde{f}(\omega) - \frac{1}{2}\tilde{g}(\omega)R^{-1}(\omega)\left[L_{\tilde{g}}V(\omega)\right]^T + L\left[y - \tilde{h}(\omega)\right]$$

$$\frac{\partial n}{\partial t} = -\frac{\partial\left[G(x,r)n\right]}{\partial r} + w(n, x, r)$$

$$\dot{x} = f(x) - \frac{1}{2}g(x)R^{-1}(\omega)\left[L_{\tilde{g}}V(\omega)\right]^T + A\int_0^{r_{\max}} a(n, r, x)dr \tag{A6}$$

Applying the method of weighted residuals to the above system, and using the notation adopted earlier, we obtain after some rearrangement, this approximate ODE system

$$\frac{d\omega}{dt} = \tilde{f}(\omega) - \frac{1}{2}\tilde{g}(\omega)R^{-1}(\omega)\left[L_{\tilde{g}}V(\omega)\right]^T + L\left[y - \tilde{h}(\omega)\right]$$

$$\dot{a}_N = f^*(a_N, x_N)$$

$$\dot{x}_N = f(x_N) - \frac{1}{2}g(x_N)R^{-1}(\omega)\left(L_{\tilde{g}}V(\omega)\right)^T + A\int_0^{\tau_{\max}} a\left[\sum_{k=1}^{N} a_{kN}(t)\phi_k(r), r, x_N\right)dr \tag{A7}$$

where the explicit expression of the nonlinear function $f^*(a_N, x_N)$ is omitted for brevity. Setting $\tilde{x} = [a_N^T \; x_N^T]^T$, we finally obtain the following closed-loop system

$$\frac{d\omega}{dt} = \tilde{f}(\omega) - \frac{1}{2}\tilde{g}(\omega)R^{-1}(\omega)\left[L_{\tilde{g}}V(\omega)\right]^T + L\left[y - \tilde{h}(\omega)\right]$$

$$\dot{\tilde{x}} = \tilde{f}(\tilde{x}) - \frac{1}{2}\sum_{i=1}^{m} \tilde{g}_i(\tilde{x})R^{-1}(\omega)L_{\tilde{g}_i}, V(\omega), \quad i = 1, \ldots, m \tag{A8}$$

Under assumptions 1, 2, and 3 stated in Theorem 1, we have already shown in the proof of Theorem 1 that there exists $\mu^* > 0$ such that if $\mu \in (0, \mu^*]$, the system is locally exponentially stable and $\lim_{t\to\infty}|y_{si} - \upsilon_i| = 0$. Using the result of proposition 1 in Chiu and Christofides (1999), we have that, for sufficiently large N, the following estimates hold

$$n(r,t) = n_N(r,t) + O(\epsilon(N))$$
$$x(t) = x_N(t) + O(\epsilon(N)) \tag{A9}$$

where $\epsilon(N)$ is a small positive real number that depends on N and satisfies $\lim_{N\to\infty}\epsilon(N) = 0$; $n_N(r,t) = \sum_{k=1}^{N} a_{kN}(t)\phi_k(r)$ is the approximation of $n(r,t)$. It follows that, for sufficiently large N, there exists positive real numbers δ_n, $\bar{\delta}_x$, δ_ω, $\bar{\mu}^*$ so that if $\mu \in (0, \bar{\mu}^*]$, $\| n(r,0) \|_2 < \delta_n, |x(0)| < \bar{\delta}_x, |\omega(0)| < \delta_\omega$, the closed-loop system of Eq. A6 is exponentially stable and $\lim_{t\to\infty}|y_i - \upsilon_i| = O[\epsilon(N)]$.

Manuscript received Aug. 2, 2000, and revision received Feb. 15, 2001.